

Fragmented superfluid due to frustration of cold atoms in optical lattices

Juan José García-Ripoll

Max-Planck-Institut für Quantenoptik, Hans-Kopfermann-Str. 1, Garching b.
München, D-85748, Germany
Universidad Complutense, Facultad de CC. Físicas, Ciudad Universitaria s/n,
Madrid E-28040, Spain

E-mail: juanjose.garciaripoll@gmail.com

Jiannis K. Pachos

Department of Applied Mathematics and Theoretical Physics, University of
Cambridge, Wilberforce Road, Cambridge CB3 0WA, UK
Quantum Information Group, School of Physics & Astronomy, University of
Leeds, Leeds LS2 9JT UK

Abstract. A one dimensional optical lattice is considered where a second dimension is encoded in the internal states of the atoms giving effective ladder systems. Frustration is introduced by an additional optical lattice that induces tunneling of superposed atomic states. The effects of frustration range from the stabilization of the Mott insulator phase with ferromagnetic order, to the breakdown of superfluidity and the formation of a macroscopically fragmented phase.

PACS numbers: 03.75.Mn, 75.10.Jm, 03.75.Lm

Submitted to: *New J. Phys.*

1. Introduction

One of the most interesting open fields in quantum magnetism is the study of frustration [1]. Frustrated models are described by Hamiltonians with competing local interactions such that the ground state cannot minimize their energy simultaneously. Frustration can appear due to the geometry of a problem, the Ising model on a triangular lattice being a paradigmatic case, or due to the coexistence of ferro- and antiferromagnetic interactions, as in spin glasses. Frustrated models typically have highly degenerate ground states, which can become ordered by increasing the temperature or by quantum fluctuations — i. e. “order by disorder”. Theoretical and numerical problems, such as the large dimensionality or the sign problem in Monte Carlo simulations make it very difficult to study frustrated Hamiltonians.

Quantum simulation has been put forward as a tool to probe the physics of a variety of many-body systems. In particular, schemes with cold atoms in optical lattices have been suggested to simulate arbitrary spin models [2, 3, 4, 5, 6, 7] and some interesting frustrated Hamiltonians [8, 9]. Compared to the alternative of looking for or inducing low-dimensional behavior on existing magnetic materials [10, 11] and in organic conductors [12, 13], the cold atoms and molecules offer greater flexibility in terms of variable geometry and interaction strength. However, the majority of current proposals are perturbative and their effective interactions are rather weak. This makes their experimental realization challenging, as it requires very low temperatures. A solution suggested to solve the problem of weak interactions is to replace the atoms with polar molecules [14].

In this paper we follow a different approach. First of all, spin up and spin down states are identified with particle and hole configurations. This gives naturally an XX coupling which is proportional to the tunneling amplitude [15] and, thus, it is strong and less experimentally demanding. By using the internal state of the atoms to encode a second virtual dimension and applying a spatially dependent Raman coupling, we are able to induce in-plane frustration. The result is a new frustrated model, which contrasts with related literature on spin ladders, where the Hamiltonian either use antiferromagnetic isotropic [16, 17, 18, 19, 20, 21] or XXZ [22] interactions, or use purely XY interactions but require a different lattice geometry [23], or both. More important, the problem we consider here is a full Bose-Hubbard Hamiltonian, and the main result is that the transport properties of the lattice change dramatically, causing the breakdown of superfluidity even for large densities in which the analogy to spin models no longer applies. In particular, in the most interesting case the Mott insulator is replaced by a new dimerized phase made, where neighboring pairs of sites have maximal coherence and there is a fast decay of coherence between pairs of sites as a function of distance. This new phase is reminiscent of a Bose glass [24], with the important difference that it has been induced by frustration and not by disorder. Our statements are supported by a variety of analytical, variational and numerical solutions.

The paper is organized as follows. In Sect. 2 we introduce the two Hubbard models that we are going to use, explain how they are implemented with cold atoms in optical lattices and briefly justify the use of the word “frustration”. In Sect. 3 we focus on a model with diagonal interactions across each square plaquette. We first discuss the different phases as obtained from DMRG calculations, including qualitative arguments about why these phases are expected. Afterwards we explain in more detail how fragmentation happens and what happens in the limit of strong interactions, and

what are the correlation properties of all available phases. In Sect. 4 we briefly present a model with frustrated rectangular lattice. In Sect. 5 we study in great detail all issues regarding the implementation of our ideas in current experiments with optical lattices. First we do a microscopic derivation of the parameters in the Hubbard Hamiltonians, including all possible sources of error. The main conclusion is that the requirements for studying these frustrated models appear to be within reach of current experiments and that there are no side-effects from introducing a Raman coupling in the experiment. We explain how the different phases studied in this paper could be detected, either from time of flight measurements or more sophisticated correlation measurements. Finally, we discuss possible sources of imperfection, such as temperature or a residual harmonic confinement. The last section (Sect. 6) contains a brief summary of our main results and possible implications and connections to other works.

2. The model

2.1. Bose-Hubbard model

The system that we are studying is that of cold atoms confined by an off-resonance optical lattice that forms a 1D bosonic lattice gas [15]. As in recent experiments [25], the lattice traps atoms in two internal states. If the confinement is strong, the effective model will be a Hubbard Hamiltonian [26]

$$H = -J \sum_{\langle i,j \rangle, \sigma} a_{i\sigma}^\dagger a_{j\sigma} + \sum_{i\sigma\sigma'} \frac{U_{\sigma\sigma'}}{2} n_{i\sigma} n_{i\sigma'} + H_R, \quad (1)$$

where J is the hopping amplitude and we assume that the on-site atomic interactions are both repulsive and symmetric, $U_{\sigma\sigma'} = U > 0$. Note that in this work, the internal state of the atoms are denoted by Greek letters, $\sigma = \uparrow, \downarrow$; the site indices are denoted by Roman characters, i, j , and go from 1 to L which is the length of the lattice; finally $N := N_\uparrow + N_\downarrow$, represents the total number of particles.

The new ingredient in our Hamiltonian are two counter-propagating laser beams that induce Raman transitions between the two atomic states. By adjusting the phase, the polarization and the alignment of these beams, we can ensure that the effective Rabi frequency, $\Omega(x)$, forms a lattice with twice the period of the confinement [Fig. 1]. We can interpret our one-dimensional system as having two 1D lattices, one for each internal state of the atom. Both chains are coupled forming a ladder thanks to both the interaction, U , and to H_R , a Raman term with the spatially dependent Rabi frequency, $\Omega(x)$.

We shall consider two specific configurations of the Raman coupling. When its maxima and minima coincide with those of the confining lattice [Fig. 1d], the result will be on-site Rabi oscillations

$$H_R = \sum_i (-1)^i J' (a_{i\uparrow}^\dagger a_{i\downarrow} + \text{H.c.}). \quad (2)$$

Alternatively, when they are displaced by half a period we will have diagonal interactions [Fig. 1a]

$$H_R = \sum_i (-1)^i J' (a_{i+1\uparrow}^\dagger a_{i\downarrow} + a_{i+1\downarrow}^\dagger a_{i\uparrow} + \text{H.c.}). \quad (3)$$

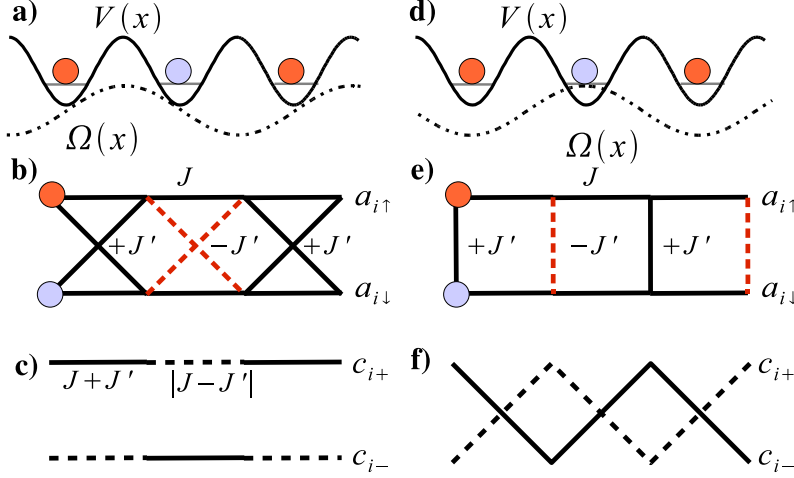


Figure 1. (a) Raman-assisted tunneling. A second optical lattice (dash-dot line) connects neighboring Wannier functions of atoms in *different* states with amplitude J' . On the other hand, normal hopping moves atoms while preserving the state, J . (b) The hard-core bosons limit resembles a spin ladder with frustrating diagonal interactions. (c) The change of variables in Eq. (5) replaces the frustrating terms with weak and strong tunnelling. (d-f) Similar drawings for the Villain model in Eq. (2).

2.2. Origin of frustration

The frustration induced by H_R becomes evident in the limit of hard-core bosons, $a_{i\sigma}^2 = 0$ [15]. Identifying the bosonic operators, $a_{i\uparrow}$ and $a_{i\downarrow}$, with the spin operators σ_{i1}^- and σ_{i2}^- , the Hamiltonian (1) becomes an XX model on a spin ladder [Fig. 1b,e]. Thus, while the hopping J translates into a ferromagnetic XX interaction along the legs, the Raman coupling H_R is a transverse XX interaction which alternates from ferro- to antiferromagnetic.

Take for instance the diagonal interactions (3). The associated spin model is

$$\begin{aligned}
 H = & \sum_{i=1,2} \sum_{j=1\dots N} J(\sigma_{ij}^x \sigma_{ij+1}^x + \sigma_{ij}^y \sigma_{ij+1}^y) + \\
 & + \sum_{j=1\dots N} (-1)^j J'(\sigma_{1j}^x \sigma_{2j+1}^x + \sigma_{1j}^y \sigma_{2j+1}^y) + \\
 & + \sum_{j=1\dots N} (-1)^j J'(\sigma_{2j}^x \sigma_{1j+1}^x + \sigma_{2j}^y \sigma_{1j+1}^y). \quad (4)
 \end{aligned}$$

The frustration arises from the competition of positive and negative contribution terms. For instance, looking at the sites $(1, j)$, $(1, j+1)$, $(2, j+1)$ and $(1, j+2)$: the bonds on this triangle have three ferro- and one antiferromagnetic terms, and there is no way in which the spins can be aligned so as to minimize the energy of all terms [see also Fig. 1b].

While the previous analogy is somewhat pleasing, one may wonder whether having more than one particle per site or working with a system which is not properly 2D will give rise to a trivial Physics. Regarding the first point, when we have more than one atom per site our model becomes equivalent to an array of Josephson junctions [9] where the frustration is still present and lays on the choice of phase for each

individual site. Regarding the second point, some of the best studied models in frustrated quantum magnetism, such as the Majumdar-Ghosh [27, 28] and the zig-zag chain [22] are also quasi-1D models. As we will show in the following sections, the competition between the different terms in Eq. (1) does indeed produce new and interesting effects with the advantage of being analytically tractable.

3. Diagonal interactions

In contrast to fully two-dimensional systems, in our quasi-1D models can be greatly simplified by rewriting the frustrated coupling using dressed states

$$c_{i\pm} := \frac{1}{\sqrt{2}}(a_{i\uparrow} \pm a_{i\downarrow}). \quad (5)$$

We will begin by studying the Raman interaction (3). With the previous change of variables, our Hamiltonian becomes

$$H = - \sum_{i;\sigma=\pm} [J + \sigma(-1)^i J'] (c_{i\sigma}^\dagger c_{i+1\sigma} + \text{H.c.}) + \frac{U}{2} n_i^2, \quad (6)$$

where $n_i := c_{i+}^\dagger c_{i+} + c_{i-}^\dagger c_{i-}$ is the total population of a single site. Eq. (6) models a ladder whose legs are made of junctions with strong, $J_+ = J + J'$, and weak hoppings, $J_- = |J - J'|$, as shown in Fig. 1c. Notice that the model is symmetric under the exchange of J and J' . In the following we will often exchange descriptions between J_+, J_- and J, J' , and we will assume, without loss of generality, that all these parameters are not negative.

3.1. Phase diagram

In this section we present zero temperature results for Hamiltonian (6). We have computed the ground states and first excitations of this model using the Density Matrix Renormalization Group (DMRG) method in the Matrix Product States (MPS) formalism [29, 30]. We have conducted accurate simulations for $L = 8, 16, 32, 50$ and 70 sites, using a cutoff of 4 particles per spin. These values give us a local dimension of the Hilbert space of 25 states, which is very big and can only be handled with state-of-the-art optimizations, such as working in sectors with well defined number of particles or angular momenta. Due to the large size of the local Hilbert space, we have typically worked with MPS of size 100 and checked convergence for different points with up to $D = 200\ddagger$. In our simulations we have computed the ground state and lowest energy states for $N/L = 1/2, 1, 5/4, 3/2, 7/4, 2$ particles, as well as the energy to add a particle, $\mu_p := E_{N+1} - E_N$, or to create a hole, $\mu_h := E_N - E_{N-1}$, and verified that these values did not change with a larger cutoff.

These zero temperature simulations reveal a very simple picture that we summarize here. As illustrated in Fig. 1d, when we increase U for fixed J_+ and J_- , the system first experiences a phase transition from a superfluid to a fragmented or dimerized phase in which coherence is maximal between pairs of neighboring sites. As the interaction is further increased these fragments evolve smoothly (i. e. a crossover)

\ddagger Note that due to our way of computing the two lowest excited states, which uses different MPS for the ground state and excitations. These simulations are comparable to DMRG calculations with $D = 300$ and $D = 600$ states, respectively, because, in the DMRG parlance, the effective basis states are optimized independently for each excited state.

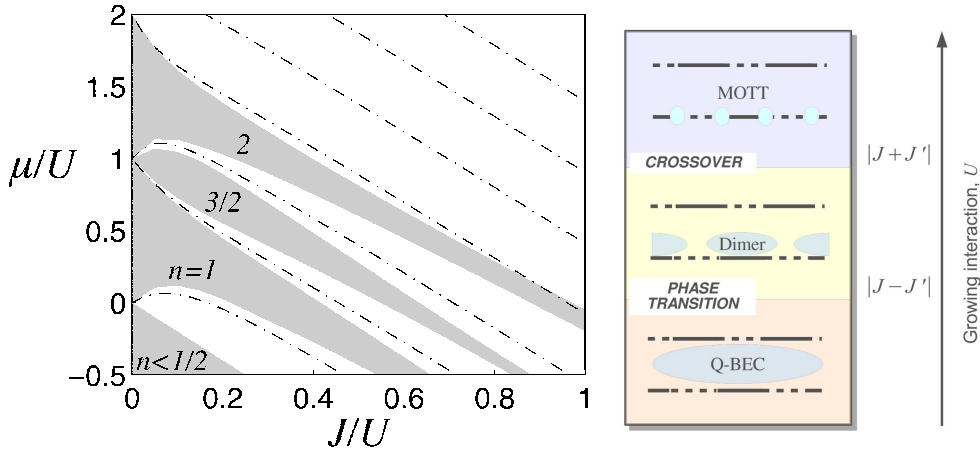


Figure 2. (left) Phase diagram for the diagonal interactions (3) computed using DMRG. For $J' = 0.9J$, the gray areas denote the incompressible Mott lobes in the space of chemical potential (μ/U) vs. hopping amplitude (J/U). The in between regions are in superfluid phase. For $J' = J$, the phase space fills with incompressible regions, each one having integer or half-integer filling, $N/L = 1, 3/2, 2, \dots$. These regions are delimited by the dash-dot lines. (right) Schema of the different phases as a function of the interaction U .

to a Mott insulator. While the first phase is gapless and its excitations are phonons, the crossover contains a gapped phase whose lowest excitations are localized spin flips.

In the following sections we will study in detail the properties of the different coupling regimes, numerically as well as analytically where possible. Nevertheless it is possible to obtain a qualitatively picture of the three regimes and the associated ground states by variational wavefunctions. First of all, for weak interactions, $U \ll J_{\pm}$, the ground state is a uniform superfluid that spread over the lattice

$$|\psi_{\text{SF}}\rangle \propto \frac{1}{\sqrt{N!}} \left[\sum_i (\alpha a_{i\uparrow}^\dagger + \beta a_{i\downarrow}^\dagger) \right]^N |\text{vac}\rangle, \quad (7)$$

with the usual rotational symmetry on the (α, β) space.

For stronger interactions, $J_- < U/4 \ll J_+$, the energy of $|\psi_{\text{SF}}\rangle$ is larger than a state made of fragmented condensates which reside on the junctions with large hopping, J_+ [Fig. 1c],

$$|\psi_{\text{frag}}\rangle \propto \prod_k (c_{2k,+}^\dagger + c_{2k+1,+}^\dagger)^{n_+} \times (c_{2k+1,-}^\dagger + c_{2k+2,-}^\dagger)^{n_-} |\text{vac}\rangle. \quad (8)$$

Here, for integer filling, $N/L = 1, 2, 3, \dots$, the ground state has is one with spontaneously broken rotational symmetry, a ferromagnetic state with either $n_+ = 0$ or $n_- = 0$. This effect arises from the contributions to the energy of both the interaction U and the hopping J_- , as it will be explained in Sect. 3.2.

Another symmetry break happens when the interactions become dominant, $U \gg J_{\pm}$. Indeed, in the limit of strongly interacting bosons and $N = L$, all ground states can be written in the form

$$|\psi_{\text{Mott}}\rangle \propto \prod_i (c_{i+}^\dagger)^{n_{i+}} (c_{i-}^\dagger)^{n_{i-}} |\text{vac}\rangle. \quad (9)$$

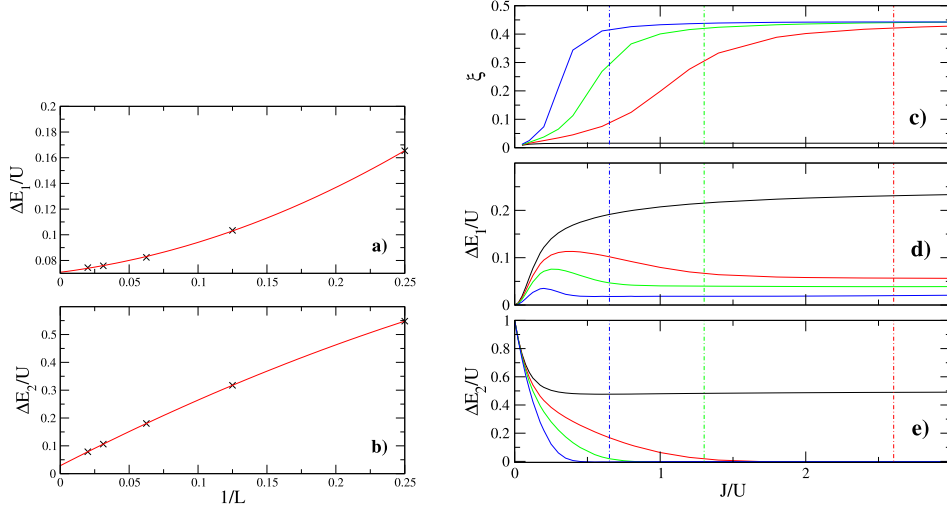


Figure 3. (a,b) Finite size scaling of the energy gaps for spin and density excitations, ΔE_1 and ΔE_2 , for a particular case $J'/U = 0.9$, $J/U = 2.8$. We fit both curves to a polynomial in $1/L$ for $L = 4, 8, 16, 32, 50$ and 70 and take the limit $1/L \rightarrow 0$. With this technique we plot in (d,e) the energy gaps vs. hopping amplitude, for $J'/J = 1.0, 0.9, 0.8, 0.6$ (top to bottom). With vertical lines we mark the points where the breakdown of superfluidity is roughly expected to take place, $U_{1D} \simeq 3.84|J' - J|$. (c) Mean correlation length, $\xi \sim \sum_{i,\delta} |\delta| \langle a_i^\dagger a_{i+\delta} \rangle / \sum_{i,\delta} \langle a_i^\dagger a_{i+\delta} \rangle$, for $J'/J = 0.6, 0.8, 0.9, 1.0$.

The quantum fluctuations generated by the hopping select, among all disordered ground states, one particular ferromagnetic state with either $n_- = 0$ or $n_+ = 0$. This case is further discussed in Sect. 3.3.

In the space of parameters, J/U , vs. chemical potential, μ , we can draw a phase diagram similar to that of the Mott-insulator transition [24]. As Fig. 2 shows, for $J' = 0.9J$, the curves of particle and hole excitations, μ_p and μ_h , create lobes (gray areas) containing fragmented phases. Crossing these lines amounts to a quantum phase transition to a superfluid, on the exterior of the lobes. Qualitatively, these lobes are similar to those of the Bose-Hubbard model [24], but about $J/|J - J'|$ times larger, so that for $J' = J$ the lobes become infinitely large and all ground states are fragmented. In this limit of $J' = J$ and for integer and half-integer filling, that is $N/L = 1, 3/2, 2, \dots$, we have on phase space infinitely many incompressible “stripes” whose borders, μ_p and μ_h , can be computed exactly [See Sect. 3.2 and Eq. (12)]. As explained above, within each stripe the state of the atoms changes smoothly from a Mott insulator (small J_+) to fragmented or dimerized phase where atoms delocalized between pairs of neighboring sites (large J_+). Interestingly, in the macrocanonical ensemble, all phases with other filling factors collapse to the lines between these regions. The large degeneracies of these other fillings has made it impossible for us to study systematically the nature of the those states and of their excitations.

To gain further insight on the properties of the ground state, let us focus on the unit filling case. The transition from the Mott phase to the superfluid is accompanied by the change of several excitation gaps. One is related to the energy required to

add or remove a particle, the other one is the energy gap required to create a density perturbation for fixed number of particles. Both gaps close at the same point when we jump from the fragmented phase to the uniform superfluid, signaling a phase transition from an incompressible to a compressible phase and also the establishment of algebraically decaying correlations [Fig. 3]. This transition occurs around the critical value of the interaction for a single-component 1D Bose-Hubbard model [31, 32, 33, 34] with hopping J_- , that is $U \sim U_{1D} := 3.84J_-$ (See Sect. 3.4). A third energy gap is present for excitations that take a particle out of one of the coherent fragments into a different spin state, while preserving the total number of particles. This gap freezes the dynamics of the spin of the atoms. As shown in Fig. 3a-b, it is maximal in the fragmented phase, with a maximum value of order $U/4$. For strong interactions it grows as J^2/U and in the superfluid phase it should close. However being $U \gg J_{pm}$ a region gapless with respect to density excitations, the DMRG simulations are probably not accurate enough to reflect this fact.

3.2. Fragmented state

In this subsection we will comment on the configurations that appear for $U \in [J_-, J_+)$. For simplicity we will begin with the case of balanced hopping and Raman coupling and no interaction, $U = J_- = 0$. Then it is trivial to see that all ground states will be of the form (8) with atoms delocalized on pairs of sites. In particular, for unit filling $N = L$ we have three degenerate states: a uniform state with all junctions populated $n_{\pm} = 1$ [Fig. 4b] and two states with broken translational symmetry, $n_- = 2$ and $n_+ = 2$ [Fig. 4a]. This degeneracy persists for small U , but it is broken as soon as we set a weak imbalance in the hoppings. For any $0 < J_- \ll U$, terms proportional to J_- connects these states off-resonantly to excited states like the ones shown in Fig. 4c-d. It follows that to second order in perturbation theory the degeneracy of these states is broken and the energy of the uniform state, $n_+ = n_-$, is shifted by an amount $\Delta E = -8(J_-^2/U) \times L$ smaller than the ferromagnetic states with broken symmetry, $\Delta E = -24(J_-^2/U) \times L$, which become the true ground state.

Once we have established that the system spontaneously selects either the c_+ or c_- order, we can compute the ground state for any value of U while keeping $J_- = 0$. Such state will be a product of ground states of the two-well problem,

$$|\psi\rangle = \prod_{i=1} | \phi^{(\bar{n})} \rangle = \prod_{i=1} \sum_{m=0}^{L/2 \bar{n}} \phi_m^{(\bar{n})} (c_{2i\sigma}^\dagger)^m (c_{2i+1\sigma}^\dagger)^{\bar{n}-m} |\text{vac}\rangle. \quad (10)$$

Here $\bar{n} = N/L = 1$ is the density, $\phi_m^{(\bar{n})}$ is the wavefunction of the double-well problem with \bar{n} atoms and $\sigma = \pm$ is the selected polarization of the atom.

To delimit the incompressible regions in phase space we only need to compute the energies of a state with $N = L, L + 1$ and $L - 1$ particles, which are variations of the one in Eq. (10). Since the ground state energies of a double well with 1, 2 and 3 particles are, respectively,

$$\begin{aligned} \epsilon_1(J_+, U) &= -2J_+, \\ \epsilon_2(J_+, U) &= \frac{U}{2} - \sqrt{\left(\frac{U}{2}\right)^2 + (2J_+)^2}, \text{ and} \\ \epsilon_3(J_+, U) &= 2U - J_+ - \sqrt{U^2 + 2UJ_+ + 4J_+^2}, \end{aligned} \quad (11)$$

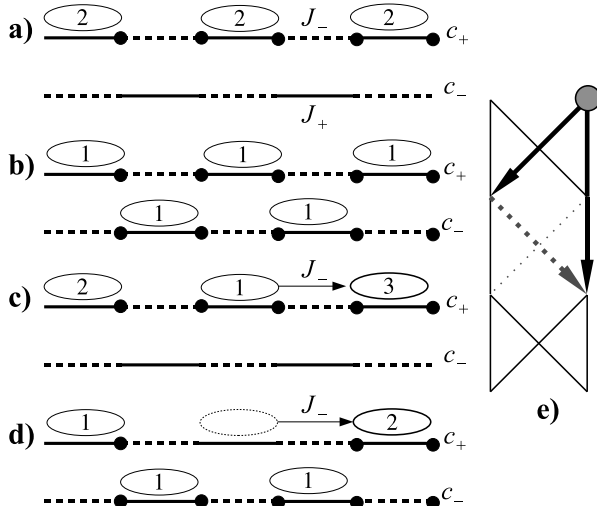


Figure 4. Two possible ground states for the fragmented phase: (a) with and (b) without spontaneous symmetry breaking. A nonzero value of J_- couples the state (a) and (b) to the excitations (c) and (d), respectively. This coupling makes the state (a) preferred for any nonzero J_- in the fragmented regime $J_- < U < J_+$. (e) A particle hopping through the lattice sees a kind of Mach-Zender interferometer. The antiferromagnetic hopping (dashed) gives rise to destructive interference on all paths longer than 2 sites.

the boundaries of the Mott region with $n = 1$ particle per site are given by

$$\begin{aligned}\mu_p(J' = J) &= \epsilon_3(2J, U) - \epsilon_2(2J, U), \\ \mu_h(J' = J) &= \epsilon_2(2J, U) - \epsilon_1(2J, U).\end{aligned}\tag{12}$$

These boundaries are the dash-dot lines we plotted in Fig. 2. A simple inspection of the previous formulas shows that these curves never cross and become parallel in the limit of $J_+/U \gg 1$.

The previous exact results, which are valid for $J_- = 0$, can be extended to $J_- \ll U, J_+$ by means of perturbation theory. In that case there will be an additional coupling between fragments up to a distance of the order of the correlation length. The wavefunction can be approximated by linear combinations of the terms (10) with different occupations of the double wells. The corrections are of order $\mathcal{O}(J_-/U)$ to the wavefunction, and of order $\mathcal{O}(J_-^2/U)$ to the energy, but the dominant term is always the one with equally populated double wells. This will be further explained in Sect. 3.4, where we analyze the location of the Mott insulator to superfluid transition. That this picture is applicable to a great degree is appreciated in Fig. 5, where we plot the correlations between different sites. For $J' = 0.9$, sites connected by J_+ are strongly correlated, while the correlations decrease significantly between different pairs of sites.

3.3. Hard-core bosons

To understand the behavior of the bosons in the strongly interacting limit, $U \gg J_{\pm}$ it is useful first to see what happens if there are no frustrating terms, $J' = 0$. We know that on the one hand, if we are below half-filling, $N < L$, the gas is a Tomonaga-Luttinger liquid with spin-charge separation [35]. In the limit of $U \rightarrow \infty$ the spin

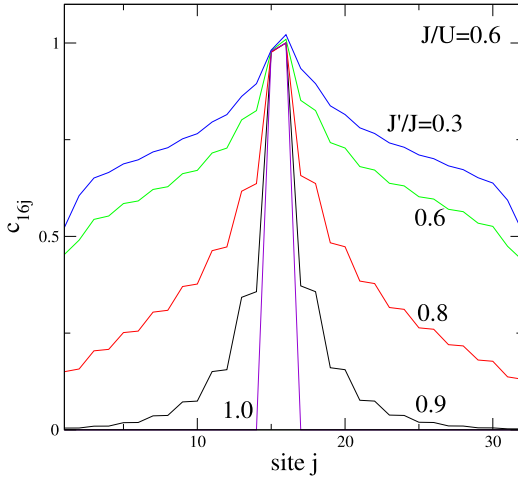


Figure 5. Correlations between different sites, $c_{i,j} := \langle c_{i+}^\dagger c_{i+} \rangle$, for $J/U = 0.6$ and $L = 32$ sites. In solid line we plot $c_{16,j}$ for different values of J'/U . For the strongly coupled sites 15 and 16, the correlations are large. For $J \simeq J'$ the correlations are dramatically reduced between sites that belong to different double wells in the effective superlattice. Note that the correlation function has period two, $c_{i,j} = c_{i+2,j+2}$, due to the superlattice structure.

degrees of freedom become degenerate and the whole system behaves like free fermions or a Tonks gas. On the other hand, for half filling, $N = L$, the sample becomes a Mott for any strong interaction $U \gg J$. The atoms cannot move but their spin degrees of freedom interact with a ferromagnetic Heisenberg interaction of strength $t = -J^2/U$ and a gapless spectrum made of spin waves.

The diagonal coupling J' changes this landscape slightly. For half filling, $N = L$, we still have a Mott phase, with one atom per site. Connecting with the previous section, as we increase U the wavefunction of the two-well fragment (10) becomes closer and closer to $\phi_m^{(\bar{n})} = \delta_{m,\bar{n}/2}$. This is a smooth evolution which is why we speak of a crossover. Furthermore, compared to the unfrustrated case $J' = 0$, the spin rotational symmetry is now broken, favoring the X direction or c_{\pm} states in the second quantization language. The effective spin model is, up to constants, a ferromagnetic one

$$H_{\text{spin}} = -\frac{1}{U} \sum_k [2J'^2 \sigma_k^x \sigma_{k+1}^x + J_+ J_- \vec{\sigma}_k \vec{\sigma}_{k+1}], \quad (13)$$

and spin excitations are prevented by an energy gap $\Delta = 2J'^2/U$ [36]. This gap is evident also in Fig. 3a, in the region of small hopping, $J \ll U$.

For smaller fillings, i. e. $N < L$, the previous spin model is no longer valid because the chain has holes. Nevertheless one can easily compute things if $J_- = 0$. The ground state manifold is composed of variations of the fragmented wavefunction (10). In particular, the set of available configurations is shown in Fig. 6, where we

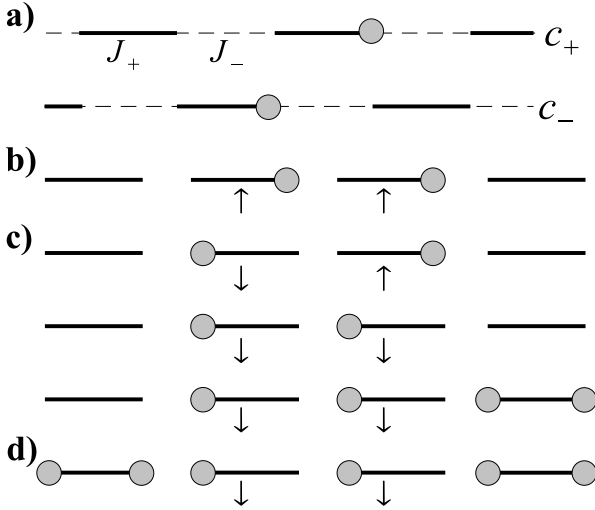


Figure 6. (a) A possible state of the ladder, where the circles denote the location of a particle. (b) The same state mapped to a 1D problem for $J_- = 0$. Allowed (b)-(c) and forbidden (d) states in the hard-core bosons limit ($U \rightarrow \infty$).

show three kinds of bonds. Those with zero or two particles, which are frozen, and bonds with one particle on the left or right sites, which can be identified with spins. These effective spins form ferromagnetic blocks which are separated by the frozen sites. If the block is surrounded by at most one doubly occupied bond, then it can only adopt one state and it has zero energy [Fig. 6d]. If the block, on the other hand is surrounded by empty blocks it may host at most one domain wall [Fig. 6c] with some small negative energy due to the motion of the domain wall (for instance, the states in Fig. 6b and Fig. 6c are connected by hopping). The effective Hamiltonian for a block of size M is

$$H_{DW} = -J \sum_{m=0}^M (|m+1\rangle\langle m| + |m\rangle\langle m+1|), \quad (14)$$

where m denotes the number of particles to the left. This gives an energy spectrum $\epsilon_k(M) = -2J \cos[k\pi/(M+2)]$, for $k = 1 \dots M+1$. Since $\epsilon_k(M)$ is a decreasing, convex function of M , the lowest energy state is achieved by making $L - N + 1$ blocks with about $N/(L - N + 1)$ atoms each. The excitations are still gapped with $\Delta \propto J$, and they can be of two types: excitations of the domain wall, and merging of two blocks. If $N < L/2$ the latter are more important and of order $\Delta = 2e_1(1) - e_1(2) \simeq 0.5858J$. On the other hand, if $N > L/2$ the excitation energy of a domain wall can be pretty small, $\mathcal{O}(1/M^2)$.

3.4. Scaling of the Mott transition

In this subsection we attempt to analyze how the superfluid to insulator transition changes due to frustration. We will do it in two different perturbative methods. The first one is based on a strong coupling expansion around $J, J' = 0$, while the second one is based on a strong coupling expansion around $J' = J$. Remarkably, this second method, which is more accurate than the trivial strong coupling expansion [33], may

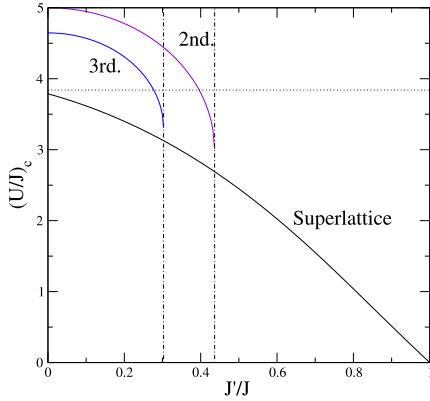


Figure 7. Critical value of U/J at which the Mott insulator to superfluid transition should take place. The blue and violet curves are based on the strong coupling expansion of third and second order in (J/U) developed in Ref. [33]. The solid line is based on a different strong coupling expansion of order $\mathcal{O}(|J-J'|^2/U)$, developed below. The dotted line is the critical value $U_c = 3.84J$ computed with DMRG for unfrustrated models [32]. Note the agreement between the two latter methods for $J' = 0$.

be contemplated as a real space renormalization technique in which the alternating Hubbard model is replaced by an effective one with a renormalized hopping and half the sites.

Our first attempt starts with the estimates of the critical value of J/U given in Ref. [33]. Applying perturbation theory up to $\mathcal{O}(J^3/U^3)$, it is possible estimate the change in the energy induced by a small amount of hopping. The resulting energies can then be used to compute the particle and hole excitation gaps, and delimit the borders of the incompressible regions in the hopping vs. chemical potential parameter space, as in Fig. 2. To apply the theory in Ref. [33] we need the hopping matrix§

$$-t_{ij} = -J_i \delta_{i+1,j} - J_{i-1} \delta_{i-1,j}, \quad (15)$$

the smallest eigenvalue of $(-t_{ij})$

$$\lambda_{\min} = -\max\{|J_+ - J_-|, |J_+ + J_-|\} = -2 \max\{J, J'\}, \quad (16)$$

the wavefunction of the single-particle ground state, $f_i = 1/\sqrt{L}$, and finally the sums

$$\sum_{ij} t_{ij}^2 f_j^2 = J_+^2 + J_-^2, \quad \sum_{ij} f_i t_{ij}^3 f_j = J_+^3 + J_-^3. \quad (17)$$

As shown in Fig. 7, the transition does indeed shift to larger values of J/U as we switch on the diagonal coupling J' . However, the prediction is not very consistent between second and third order expansions, and it even fails to provide the right value for $J' = 0$, probably due to the asymptotic nature of these expansions.

Our second attempt focuses on the regime of strong frustration or values of J' close to J . We have seen that for $J' = J$ the incompressible regions fill the entire phase

§ We assume periodic boundary conditions.

space. With very simple arguments it is possible also to compute how they shrink for nonzero $|J' - J| = \epsilon \ll U$. The reasoning begins by noticing that our system is a superlattice, where the weak hopping terms can be treated perturbatively. However, instead of using the Mott states as unperturbed states one must use the exact ones for $J_+ > 0$. Basically, we have an unperturbed state with energy $E = L\epsilon_2/2$ and several unperturbed manifolds above it, consisting on holes and excitations in the superlattice, with energy gaps of order $\epsilon_3 - \epsilon_2$, $\epsilon_1 - \epsilon_2$. We can compute the corrected μ_p and μ_h as a function of J_- . The equation for the critical point then looks as follows

$$\mu_p - \mu_h = \epsilon_3(U) + \epsilon_1(U) - 2\epsilon_2(U) - J_-c(U) + \mathcal{O}(J_-^2) = 0, \quad (18)$$

where the energies and the matrix elements of the hopping Hamiltonian, $c(U)$, are functions of U . We have solved numerically the highly nonlinear equation (18) for U as a function of J_- and J_+ . The results are plotted in Fig. 7. As seen there, this second method interpolates properly between the critical value of $U = 3.84$ obtained by DMRG for the unfrustrated model [32], and the critical value $U = 0$ computed for $J = J'$. Furthermore, the whole line deviates very little from $U_c = U_c(J' = 0)|J - J'|$.

3.5. Correlators

As it will be useful to identify the different phases experimentally, we have computed the single-body and two-body correlation functions in the three regimes. The most interesting values are the single-body correlators, $\langle a_i^\dagger a_j \rangle$. In the superfluid limit, due to the one-dimensional character of our problem, we expect that correlations decay algebraically. In the fragmented regime, we have two possible ground states, depending on whether the fragments sit on even or odd junctions, which is equivalent to specify whether the fragments are made of c_+ or c_- particles. In the first case we will have

$$\langle c_{2i,+}^\dagger c_{2i,+} \rangle = \langle c_{2i,+}^\dagger c_{2i+1,+} \rangle = \langle c_{2i,+}^\dagger c_{2i,+} \rangle = 1/2, \quad (19)$$

with all other correlators being zero, and in the c_- case we will have the same correlation pattern but displaced by one lattice site. Finally, in the Mott insulator regime we have no correlations and $\langle c_{i\pm}^\dagger c_{j\pm} \rangle_{\text{frag}} \sim \delta_{i-j}$.

In experiments what is measured is the time of flight images. These pictures are related to the momentum distribution of the sample or the Fourier transform of the single-particle correlations

$$n_q \propto \sum_{k,l=1}^L e^{i2\pi q(k-j)/L} \langle a_k^\dagger a_j \rangle \quad q \in [-L/2, L/2]. \quad (20)$$

This function is peaked at $q = 0$ and decays towards the sides of the Brillouin zone. The half-width of the peak is related to the correlation length of the sample. In the superfluid region it will be proportional to the size of the lattice and limited by finite temperature effects [37]. As soon as we cross the phase transition towards the fragmented phase, though, the correlation length decays abruptly to $\xi = 2$ sites and the previous function has a constant width

$$n_q \sim 1 + \cos(2\pi q/L) \quad (21)$$

From there on we expect a smooth crossover towards $n_q = 1$ which is the Mott-Insulator regime. All this phenomenology is evident in Fig. 9.2

4. Villain model

The other limiting case in our setup is that of vertical frustrating interactions, a configuration resembling the *odd model* or Villain lattice [1]. Once more it is convenient to change basis as in Eq. (5), so that the frustrating terms become alternating energy shifts

$$H = \sum_{i;\sigma=\pm} \left[-J(c_{i\sigma}^\dagger c_{i+1\sigma} + \text{H.c.}) - (-1)^i \sigma J' c_{i\sigma}^\dagger c_{i\sigma} + \frac{U}{2} n_i^2 \right]. \quad (22)$$

The effect of the Raman coupling is now equivalent to a superlattice. This additional potential splits the Wannier band into two effective bands separated by a gap J' , each band having a reduced width $\Delta J := (\sqrt{4J^2 + J'^2} - J)/2$. The superlattice localizes the atoms on alternating rungs, forming an antiferromagnetic configuration. Instead of exhibiting fragmentation, the system goes straight from a superfluid to a Mott-insulator, but now the transition happens for weaker interactions, $U \sim \Delta J$.

5. Experimental realization

There are several issues that one has to consider when implementing our Hubbard models using neutral atoms. The first one is how to relate U , J and J' with experimental parameters such as the intensity of the Raman laser and the strength of the optical lattice. Additionally one has to consider how to prepare the ground state and how cold the sample should be. Finally one has to think about procedures to detect the different phases. We will address all of these questions in the following sections.

5.1. Microscopic theory of Hubbard model

In this subsection we show how to derive the constants U , J and J' using a band structure calculation that takes into account the Raman coupling, $\Omega(x) = \Omega_0 \cos(kx + \phi)$, and the confining lattice,

$$V(x) = V_{0x} \sin(kx)^2 + V_{0\perp} [\sin(ky)^2 + \sin(kz)^2]. \quad (23)$$

Our work generalizes the ideas from Ref. [26], but now our microscopic Hamiltonian

$$H = \sum_{\sigma,\sigma'} \int d\mathbf{x} \psi_{\sigma'}^\dagger(\mathbf{x}) \left[-\frac{\hbar^2}{2m} \nabla^2 + W_{\sigma\sigma'}(\mathbf{x}) \right] \psi_{\sigma'}(\mathbf{x}) \quad (24)$$

contains a potential term

$$W_{\sigma\sigma'} = V(\mathbf{x}) \delta_{\sigma\sigma'} + \Omega(\mathbf{x}) \delta_{\sigma\bar{\sigma}'} + \sum_{\alpha=\uparrow,\downarrow} \frac{\tilde{U}_{\sigma\alpha}}{2} |\psi_\alpha(\mathbf{x})|^2 \quad (25)$$

that includes not only the trapping potential, but the coupling and the interaction between atomic states.

Following [26], we perform a tight-binding approximation and replace the bosonic operator by an expansion of the form

$$\psi(\mathbf{x}) \simeq \sum_{i,j,k,\sigma} a_{ijk\sigma} w_x(x - bi) w_y(y - bj) w_z(z - bk), \quad (26)$$

where $b = \pi/k$ is the period of the lattice and $w_{x,y,z}$ are the Wannier function corresponding to the lowest Bloch band of the lattice, along the X, Y and Z directions,

respectively. By substituting this expansion into the full Hamiltonian (24) and retaining the most important terms, one arrives to a Bose-Hubbard model (1).

To compute the parameters of our model, we will assume that the confinement along the transverse directions, $V_{0\perp}$, is big enough, so that hopping is negligible and our system is made of multiple, disconnected 1D lattices. However, even with this assumption there are still too many “knobs” to tune. To simplify the problem it is customary to adimensionalize all magnitudes using the energy of the lattice, $E_R = \hbar^2 k^2 / 2m$, and its period, b , as units. We replace the trapping potential with $V \sim V_0 \cos(2kx)$, make the change of variables $2kx \rightarrow 2\pi x$ and rescale the wavefunction accordingly, $w \rightarrow w\sqrt{k/\pi}$. As a result we obtain formulas for the hopping

$$\frac{J}{E_R} = \int dx w_x(x+1) \left[-\frac{1}{\pi^2} \frac{d^2}{dx^2} + \frac{V_0}{2E_R} \cos(x) \right] w_x(x), \quad (27)$$

the Raman coupling

$$\frac{J'}{E_R} = \int \frac{\Omega_0}{E_R} \cos(\pi x + \phi) |w_x(x)|^2 dx, \quad \phi \in \{0, \pi/2\} \quad (28)$$

and the interaction energy

$$\frac{U_{\sigma\sigma'}}{E_R} = a_{\sigma\sigma'}^{(1D)} \int dx |w_x(x)|^4 =: a_{\sigma\sigma'}^{(1D)} I(V_0/E_R). \quad (29)$$

Notice that $w_x(x)$ is now a Wannier function computed for a single, one-dimensional problem with period 2π and trapping V_0/E_R . The only other free parameters are Ω_0/E_R , and the effective one-dimensional scattering length ||

$$a_{\sigma\sigma'}^{(1D)} := \frac{4}{\pi^2} k a_{\sigma\sigma'}^{(3D)} I(V_{0\perp}/E_R)^2. \quad (30)$$

At this point one has to solve a family of one-dimensional problem with the periodic potential $\cos(2\pi x)$ in order to obtain the relative values of J, J' and U .

5.2. Experimental parameters

From the computations sketched in Sect. 5.1, it follows that if we choose the Rabi coupling of similar strength to the confinement, $\Omega_0 = V_0/2$, then the ordinary hopping, J , and the ladder coupling, J' , are also of the same order of magnitude [Fig. 8]. That means that by slightly tuning Ω_0 it should be experimentally feasible to cover all possible regimes, from $J_- = J_+$ to $J_- = 0$.

Now it only remains the question of whether we can make U/J small or big enough to explore the different phases. For a typical experiment with ^{87}Rb , we have $a^{3D} \sim 5\text{nm}$ and the wavelength of the laser is $\lambda \sim 850\text{nm}$, so that $a_{\sigma\sigma'}^{(1D)} \sim 1.8 \times 10^{-3} I^2$. Now, for a strong confinement we have that I ranges from 2 to 8, and comparing with the evolution of J and J' in Fig. 8 we see that the value of the interaction can indeed change from a superfluid regime, $U < |J - J'|$, to the Mott insulator regime, $|J + J'| \ll U$. In other words, if we keep $J - J'$ not too small, the laser intensities will not differ much from those used in current experiments [15, 39] and we will be able to generate all phases.

While the validity of the tight-binding approximation is well established for the ordinary Bose-Hubbard model, we have introduced a coupling between neighboring

|| Note that this is an effective value, unrelated to the scattering theory of cold atoms in 1D tubes by Olshanii [38].

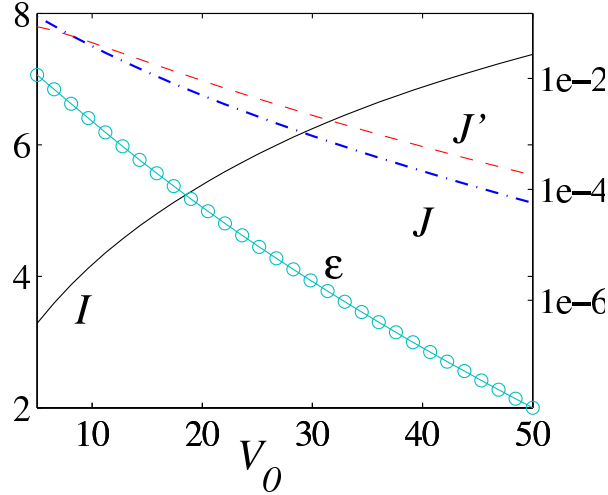


Figure 8. Parameters of the model, I (solid, left axis), J (dash-dot, right) and J' (dashed, right) as a function of the lattice depth, V_0 , for a Rabi coupling $\max|\Omega(x)| = V_0/2$, and diagonal interactions, $\phi = \pi/2$. The value ϵ (circles, right) is the effective coupling to higher bands (31). All parameters are measured in units of the recoil energy of the confining lattice.

sites that might excite the atoms to higher Bloch bands. We have studied this effect and computed the following effective strength of the coupling

$$\epsilon := \left| \frac{\max |Q_i(\Omega_0/E_R)|}{\Delta E} \right|^2, \quad (31)$$

which is a function of the energy difference between bands, ΔE , and the coupling between Wannier functions of the lowest and first excited bands

$$Q_i(\Omega_0/E_R) := \frac{\Omega_0}{E_R} \int w_x(x) \cos(x/2 + \phi) w_x^{(2)}(x-i). \quad (32)$$

When small, the value ϵ measures how much mixing of the excited wavefunctions there is in the ground state and it is a function of Ω_0 . As Fig. 8 shows, for the diagonal interactions ($\phi = \pi/2$) the coupling is indeed extremely small, $\epsilon < 10^{-2}$, and we can be sure that our approximations are valid. Similar results are obtained for $\phi = 0$.

5.3. Preparation and observation

The remaining issues are related to the possibility of preparing and unambiguously identifying the ground states of our model (1). The state preparation can be done in a two step process. One begins with a 1D superfluid and all atoms in the same internal state, and slowly increasing the lattice depth. Judging from current experiments, this should be a robust way to create a Mott or Tonks gas phase [15]. For $U \gg J, J'$ the density excitations will be frozen and the dynamics will be ruled by the effective ferromagnetic model (13). One can then slowly increase J' to create the ground state of (13) which will be the ground state of the frustrated model.

Regarding detection, the three phases of model (3) can be identified from time of flight images. First of all, for $U \ll J_{\pm}$ we expect a quasi-condensate which will produce strong interference peaks in either of the atomic species. The width of these peaks may

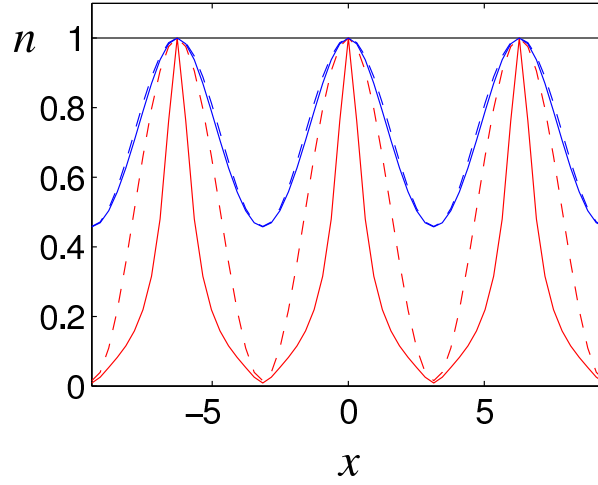


Figure 9. Ideal interference pattern arising from time of flight images of the model with diagonal interactions (3). We show results for $N = L = 32$ particles, $J/U = 0, 0.05$ and 0.5 , from top to bottom, using $J' = J$ (dash) and $J' = 0.9J$ (solid). See Sect. 5.3 for details about n and x .

be slightly modified by temperature [37] but it should remain approximately constant for $U < J_{\pm}$. For moderately strong interactions, $J_- < U < J_+$, the correlation length will decrease substantially as we expect coherences only inside each fragment. Thus according to Sect. 3.5 the interference pattern will be approximately

$$|\psi(tp/m)|^2 \sim |\tilde{w}(p)|^2 [1 + \cos(p)] =: |\tilde{w}(p)|^2 n(p). \quad (33)$$

Here $\tilde{w}(p)$ is the Fourier transform of a Wannier wavefunction, n is the ideal interference pattern and the position $x = tp/m$ is related to the time, t , the mass of the atoms, m , and its momentum in the lattice, p . In practice, for $J' \neq J$, the remaining coherence between fragments can modify this pattern, giving thinner peaks, as shown in Fig. 9.

Another signature of the transition from quasi-condensate to fragmented phase is a spontaneous symmetry break that makes the ground state be formed of either c_+ or c_- particles. The energy gap in this phase is related to the stiffness of the atoms with respect to a change in the internal state and it could be probed spectroscopically.

A third signature which applies to both the fragmented phases and the ground state of the Villain model is the existence of magnetic order. More precisely, for strong interactions $J_+ < U$, the ground states of the diagonal and Villain frustrated models have ferro- and antiferromagnetic order, respectively. This pattern reveals itself in high order correlations between the number of atoms of c_+ and c_- at different sites: $\langle c_{j\sigma}^\dagger c_{j\sigma'} c_{i\sigma}^\dagger c_{i\sigma'} \rangle \propto 1 + \epsilon \sigma \sigma' (-1)^{i-j}$, where $\epsilon = 1$ or 0 for each model, respectively. To observe these correlations one must first rotate the atoms with a $\pi/2$ pulse, as in Eq. (5), and afterwards analyze the quantum fluctuations in the time of flight images [40]. Alternatively, if the experiment allows for state dependent lattices and photo-association, it will be advantageous to use the techniques suggested in [7] to measure the number correlations. This second method should indeed provide a much stronger signal.

In current experiments we have to consider two additional sources of imperfection that can influence our observations. One of them is the residual harmonic confinement

which is always present due to the difference on intensity along the lasers that trap the atoms. From the diagram of Fig. 2, the harmonic confinement will cause the atomic cloud to be made of nested insulating shells with different densities [26], while the size of the superfluid regions will substantially decrease and strictly vanish for $J = J'$. This structure can cause noise in the interference patterns, but, as it has been shown in recent experiments [41], it can also be probed using RF knives and spin-changing collisions.

The second source of imperfections is temperature, which will influence the measurements in two ways. First of all, for $T \neq 0$, the weakly interacting region will not be a condensate, but a quasi-condensate, where phase fluctuations are energetically cheap but the system remains superfluid. One might argue that these phase fluctuations will destroy the interference peaks, but as we have seen in 1D experiments with optical lattices [39], this does not seem to happen in practice. Moreover, the correlation length of the quasi-condensate will be much larger than that of the fragmented phase, a fact that will be evident in the interference pattern. It remains the question of whether the fragmented phase itself is robust against temperature and we argue that indeed it is. This phase will be observed if the temperature of the system is smaller or comparable to the energy gap, Δ . But as shown in Fig. 3 the energy gap can be considerably large, $\Delta \sim 0.6J$, sufficiently larger than the temperature limitations of the latest experiments [15, 41]. We expect that under these conditions the fragmented phase can be unambiguously identified.

6. Conclusions

In this work we have introduced several new ideas. The first one is to use internal states of atoms in an optical lattice to simulate additional spatial dimension and to implement ladders. While it may be argued that there are previous works which have actively employed the internal degrees of freedom of the atom for quantum simulation [42, 43, 2, 4, 6, 7], it is in this work that they are used to effectively increase the dimensionality of the lattice.

The second idea is to couple the atomic degrees of freedom in a spatially dependent way [42], so as to induce a frustrating hopping in the new virtual dimensions. The frustrating nature if this assisted tunneling arises from the sign of the Raman coupling and it is best appreciated in the hard-core bosons limit, in which the model is tantamount to a spin Hamiltonian [Sect. 2.2]. Additionally, this frustrating hopping can also be seen as originating multiple small Mach-Zender interferometers in the lattice, such that destructive interference disturb the motion of atoms along the lattice [Fig. 4e].

The most dramatic consequence of these two kinds of tunneling is the breakdown of superfluidity. The ground state fragments into a macroscopic number of double-well subsystems which lose coherence among them as we increase the strength of interactions. This situation is reminiscent of a Bose glass where a disordered energy landscape creates islands of superfluid regions with no coherence among them [24]. However, in our case the fragmentation is induced by frustration and not by disorder.

It is possible to qualitatively connect the Physics observed here with that of other spin models. On the one hand, the modulation of the hopping leads to an effective superlattice in the internal plus motional degrees of freedom. This superlattice gives rise to a larger coherence between neighboring lattice sites, similar to what happens in the spin-Peierls effect, where a modulation of a Heisenberg interaction leads to

dimerization [44]. Thus, in contrast to other models where dimerization happens spontaneously [22], here it is imposed by the quantum interference of hopping terms.

However, while this analogy to spin models explains the fragmentation, our system goes beyond this simple picture, since we actually have two superlattices which are connected by repulsive interactions. The internal degrees of freedom of the atoms give rise to rich Physics both in the strongly repulsive regime and in the insulator to superfluid transition. In particular, the dynamics of the spin deep in the superfluid region deserve to be studied in future work.

The methods shown here can be applied to simulating spin ladders as the ones studied in Ref. [7]. Additionally, the internal degrees of freedom of the atoms can be used to change the topology of the lattice from square to triangular. Finally, a natural extension would be to combine the Raman coupling used here with a two-dimensional or even a three-dimensional optical lattice, so as to simulate new topologies and other frustrated bilayer magnetic models that may have not been considered so far.

References

- [1] H. T. Diep, editor. *Frustrated Spin Systems*. World Scientific, Singapore, 2004.
- [2] E. Jané, G. Vidal, W. Dürr, P. Zoller, and J. I. Cirac. Simulation of quantum dynamics with quantum optical systems. *Quant. Inf. Comp.*, 3:15, 2003.
- [3] A. B. Kuklov and B. V. Svistunov. Counterflow superfluidity of two-species ultracold atoms in a commensurate optical lattice. *Phys. Rev. Lett.*, 90:100401, 2003.
- [4] L.-M. Duan, E. Demler, and M. D. Lukin. Controlling spin exchange interactions of ultracold atoms in optical lattices. *Phys. Rev. Lett.*, 91:090402, 2003.
- [5] J. J. García-Ripoll and J. I. Cirac. Spin dynamics for bosons in an optical lattice. *New Journal of Physics*, 5:76, 2003.
- [6] S. K. Yip. Dimer state of spin-1 bosons in an optical lattice. *Phys. Rev. Lett.*, 90:250402, 2003.
- [7] J. J. García-Ripoll, M. A. Martín-Delgado, and J. I. Cirac. Implementation of spin hamiltonians in optical lattices. *Phys. Rev. Lett.*, 93:250405, 2004.
- [8] L. Santos, M. A. Baranov, J. I. Cirac, H.-U. Everts, H. Fehrmann, and M. Lewenstein. Atomic quantum gases in kagomé lattices. *Phys. Rev. Lett.*, 93:030601, 2004.
- [9] Marco Polini, Rosario Fazio, A. H. MacDonald, and M. P. Tosi. Realization of fully frustrated josephson-junction arrays with cold atoms. *Physical Review Letters*, 95(1):010401, 2005.
- [10] Sudha Gopalan, T. M. Rice, and M. Sigrist. Spin ladders with spin gaps: A description of a class of cuprates. *Phys. Rev. B*, 49(13):8901–8910, Apr 1994.
- [11] M. Azuma, Z. Hiroi, M. Takano, K. Ishida, and Y. Kitaoka. Observation of a spin gap in SrCu_2O_3 comprising spin-1/2 quasi-1d two-leg ladders. *Phys. Rev. Lett.*, 73(25):3463–3466, Dec 1994.
- [12] Joel S. Miller and Arthur J. Epstein. Organic and organometallic molecular magnetic materials-designer magnets. *Angewandte Chemie International Edition in English*, 33:385–415, 1994.
- [13] A. M. S. Macêdo, M. C. dos Santos, M. D. Coutinho-Filho, and C. A. Macêdo. Magnetism and phase separation in polymeric hubbard chains. *Phys. Rev. Lett.*, 74(10):1851–1854, Mar 1995.
- [14] A. Micheli, G. K. Brennen, and P. Zoller. A toolbox for lattice-spin models with polar molecules. *Nature Physics*, 2:341–347, May 2006.
- [15] Belén Paredes, Artur Widera, Valentin Murg, Olaf Mandel, Simon Fölling, Ignacio Cirac, Gora V. Shlyapnikov, Theodor W. Hänsch, and Immanuel Bloch. Tonks-girardeau gas of ultracold atoms in an optical lattice. *Nature*, 429:277–281, 2004.
- [16] Hsiang-Hsuan Hung, Chang-De Gong, Yung-Chung Chen, and Min-Fong Yang. Search for quantum dimer phases and transitions in a frustrated spin ladder. *Physical Review B (Condensed Matter and Materials Physics)*, 73(22):224433, 2006.
- [17] Temo Vekua and Andreas Honecker. Quantum dimer phases in a frustrated spin ladder: Effective field theory approach and exact diagonalization. *Physical Review B (Condensed Matter and Materials Physics)*, 73(21):214427, 2006.
- [18] Dave Allen, Fabian H. L. Essler, and Alexander A. Nersisyan. Fate of spinons in spontaneously dimerized spin- $\frac{1}{2}$ ladders. *Phys. Rev. B*, 61(13):8871–8877, Apr 2000.
- [19] Eugene H. Kim, G. Fáth, J. Sólyom, and D. J. Scalapino. Phase transitions between topologically distinct gapped phases in isotropic spin ladders. *Phys. Rev. B*, 62(22):14965–14974, Dec 2000.

- [20] Alexander A. Nersisyan, Alexander O. Gogolin, and Fabian H. L. Eßler. Incommensurate spin correlations in spin- 1/2 frustrated two-leg heisenberg ladders. *Phys. Rev. Lett.*, 81(4):910–913, Jul 1998.
- [21] Martin P. Gelfand. Linked-tetrahedra spin chain: Exact ground state and excitations. *Phys. Rev. B*, 43(10):8644–8645, Apr 1991.
- [22] F. D. M. Haldane. Spontaneous dimerization in the $s = \frac{1}{2}$ heisenberg antiferromagnetic chain with competing interactions. *Phys. Rev. B*, 25(7):4925–4928, 1982.
- [23] T. Hakobyan, J. H. Hetherington, and M. Roger. Phase diagram of the frustrated two-leg ladder model. *Phys. Rev. B*, 63(14):144433, Mar 2001.
- [24] M. P. A. Fisher, Peter B. Weichman, G. Grinstein, and D. S. Fisher. Boson localization and the superfluid-insulator transition. *Phys. Rev. B*, 40:546–570, 1989.
- [25] Artur Widera, Olaf Mandel, Markus Greiner, Susanne Kreim, Theodor W. Hansch, and Immanuel Bloch. Entanglement interferometry for precision measurement of atomic scattering properties. *Phys. Rev. Lett.*, 92(16):160406, 2004.
- [26] D. Jaksch, C. Bruder, J. I. Cirac, C. W. Gardiner, and P. Zoller. Cold bosonic atoms in optical lattices. *Phys. Rev. Lett.*, 81:3108–3111, 1998.
- [27] Chanchal K. Majumdar and Dipan K. Ghosh. On next-nearest-neighbor interaction in linear chain. i. *Journal of Mathematical Physics*, 10(8):1388–1398, 1969.
- [28] Chanchal K. Majumdar and Dipan K. Ghosh. On next-nearest-neighbor interaction in linear chain. ii. *Journal of Mathematical Physics*, 10(8):1399–1402, 1969.
- [29] Frank Verstraete, Diego Porras, and Juan Ignacio Cirac. Density matrix renormalization group and periodic boundary conditions: A quantum information perspective. *Phys. Rev. Lett.*, 93:227205, 2004.
- [30] Ingo Peschel, Xiaogun Wang, and Matthias Kaulke, editors. *Density-Matrix Renormalization*. Springer, Berlin, 1999.
- [31] S. Rapsch, U. Schollwöck, and W. Zwerger. Density matrix renormalization group for disordered bosons in one dimension. *Europhysics Letters (EPL)*, 46(5):559–564, 1999.
- [32] T. D. Kühner and H. Monien. Phases of the one-dimensional bose-hubbard model. *Phys. Rev. B*, 58(22):R14741–R14744, Dec 1998.
- [33] J. K. Freericks and H. Monien. Strong-coupling expansions for the pure and disordered bose-hubbard model. *Phys. Rev. B*, 53(5):2691–2700, Feb 1996.
- [34] Richard T. Scalettar, Ghassan George Batrouni, and Gergely T. Zimanyi. Localization in interacting, disordered, bose systems. *Phys. Rev. Lett.*, 66(24):3144–3147, Jun 1991.
- [35] J. Voit. One-dimensional fermi liquids. *Reports on Progress in Physics*, 58(9):977–1116, 1995.
- [36] T. Koma and B. Nachtergaele. The spectral gap of the ferromagnetic xxz chain. *Lett. Math. Phys.*, pages 1–16, 1997.
- [37] M A Cazalilla, A F Ho, and T Giamarchi. Interacting bose gases in quasi-one-dimensional optical lattices. *New Journal of Physics*, 8(8):158, 2006.
- [38] M. Olshanii. Atomic scattering in the presence of an external confinement and a gas of impenetrable bosons. *Phys. Rev. Lett.*, 81(5):938–941, Aug 1998.
- [39] Thilo Stoferle, Henning Moritz, Christian Schori, Michael Kohl, and Tilman Esslinger. Transition from a strongly interacting 1d superfluid to a mott insulator. *Physical Review Letters*, 92(13):130403, 2004.
- [40] Simon Fölling, Fabrice Gerbier, Artur Widera, Olaf Mandel, Tatjana Gericke, and Immanuel Bloch. Spatial quantum noise interferometry in expanding ultracold atom clouds. *Nature*, 434:481–484, 2005.
- [41] Simon Fölling, Artur Widera, Torben Muller, Fabrice Gerbier, and Immanuel Bloch. Formation of spatial shell structure in the superfluid to mott insulator transition. *Physical Review Letters*, 97(6):060403, 2006.
- [42] D. Jaksch and P. Zoller. Creation of effective magnetic fields in optical lattices: the hofstadter butterfly for cold neutral atoms. *New Journal of Physics*, 5:56, 2003.
- [43] K. Osterloh, M. Baig, L. Santos, P. Zoller, and M. Lewenstein. Cold atoms in non-abelian gauge potentials: From the hofstadter "moth" to lattice gauge theory. *Physical Review Letters*, 95(1):010403, 2005.
- [44] Thierry Giamarchi. *Quantum Physics in One Dimension*. Oxford Univ. Press, Oxford, 2004.